THE JOURNAL OF PHYSICAL CHEMISTRY C

pubs.acs.org/JPCC Article

Nonadiabatic Dynamics at the Gas−Molten Metal Interface: State-to-State Resolved Scattering of NO from Hot Gallium (600−1000 K)

Amelia Zutz, Kirk A. Peterson, and David J. Nesbitt*

Cite This: J. Phys. Chem. C 2021, 125, 341−353 Read Online

ACCESS | Metrics & More | Article Recommendations | Supporting Information

ABSTRACT: This work reports the first quantum-state-resolved collisional energy-transfer studies of supersonically cooled NO colliding with the surface of hot, molten Ga and detected by laser-induced fluorescence on the $A^2\Sigma^+(v = 0) \leftarrow X^2\Pi(v = 0, 1)$ electronic transition band. The studies are performed at both low (E_{inc} = 2.0(7) kcal/mol) and hyperthermal (E_{inc} = 20(2) kcal/mol) collision energies and as a systematic function of the gas−molten metal interfacial temperature (600−1000 K). The results provide evidence for efficient rotational and spin−orbit excitation, the latter of which signals the presence of nonadiabatic surface hopping dynamics. Furthermore, the temperature-dependent studies also yield direct evidence for efficient vibrational excitation of NO at a gas−molten metal interface, in remarkably close agreement with studies of NO scattering from hot molten Au. Of particular dynamical relevance, this vibrationally inelastic scattering efficiency closely follows Arrhenius behavior, with an activation energy (E_a = 1850 (130) cm^{-1}) in quantitative agreement with the NO(v = 1 ← 0) energy spacing of 1876 cm^{-1}. This behavior provides confirmation for significant contributions from a nonadiabatic excitation mechanism, whereby a continuum of thermally populated electron−hole pair states in the molten Ga metal facilitates resonant energy transfer from the metal to the NO. This is also entirely consistent with models proposed by Tully, Wodtke, and co-workers for the inverse scattering process, namely, efficient multiquantum relaxation of NO(v) by collisions with single-crystal Au(111), postulated to occur via transient electron transfer from the metal surface to form a temporary NO^- ($^3\Sigma^+$) anion. In further support of this model, we present high-level ab initio calculations at the CASSCF/AVnZ (n = 3, 4) level for the simplest Ga−NO cluster, yielding direct evidence for significant electron transfer from Ga to NO as a function of Ga−N interatomic distance.

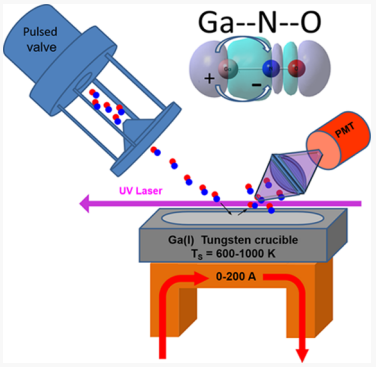

I. INTRODUCTION

Electronically nonadiabatic interactions have been investigated extensively in molecular collisions with solid metallic surfaces,[1−10] with quantum-state-resolved details of energy transfer between gas-phase molecules at molten metals much less well understood. The conduction band of a metal consists of a continuum of infinitesimally spaced electronic states, from which an electron−hole pair can be formed when an electron is excited above the Fermi level, thus creating a hole in the conduction band. Because these electronic energies constitute a true continuum, any rovibronic excitation in a molecule colliding with the solid or molten metallic surface can isoenergetically form an electron−hole pair state, thereby always ensuring a pathway for resonant energy relaxation into the gas−metal interface. The inverse of this mechanism, i.e., resonant excitation of an incident molecule by thermally populated electron−hole pair states, similarly comprises an intrinsically nonadiabatic electronic process, whereby electronic degrees of freedom in the metal couple strongly to rovibronic degrees of freedom in the adsorbate.[1,11−13]

As one well-studied system, a number of classic experiments have investigated how nitric oxide (NO) transfers vibrational energy to/from a variety of single-crystal metals, providing evidence for electron−hole pair-mediated vibrational and electronic energy transfer at the NO−metal interface.[1] For example, Wodtke and co-workers beautifully demonstrated that molecular beams of vibrationally excited NO(v = 15) scatter from Au(111), with an average loss of $\Delta v \sim 8$ quanta observed in the scattered flux.[9] By way of clear contrast, however, when NO(v = 12) was scattered from an insulating LiF surface,[7] vibrational relaxation was found to be almost entirely absent, which was attributed to the lack of electron−hole pair states resonant with Δv energy-level differences in the incoming NO molecule. These results provided compelling first evidence that interactions with the conductive metal surface are responsible for multiquanta vibrational relaxation. Additional experiments tested and confirmed these ideas, investigating vibrationally mediated electron emission from Au(111) with a layer of Cs, which lowers the work function of the surface down to 1.6 eV.[10] In these studies, NO molecules

Received: August 28, 2020
Revised: December 3, 2020
Published: December 29, 2020

https://dx.doi.org/10.1021/acs.jpcc.0c07861
J. Phys. Chem. C 2021, 125, 341−353

were directed at the surface over a range of incident vibrational states, with direct ejection of electrons into vacuum only observed when the incident NO vibrational energy exceeded the work function (ϕ) of the surface. This entire body of results provided support for strong nonadiabatic coupling of molecular vibrational motion to conduction electrons in the metal, representing a fundamental breakdown of the Born−Oppenheimer approximation.[14−17]

Such observations of nonadiabatic NO($v \leftarrow v''$) vibrational energy-transfer dynamics have not been isolated to Au(111). Indeed, numerous experiments dating back to the mid-1980s have observed vibrational excitation of NO scattered from other single-crystalline metal surfaces.[1,11,13,18−21] Of particular interest, many of these experiments also demonstrated simple Arrhenius behavior for the dependence of vibrational excitation probability on surface temperature,[1,13,18,21] with an Arrhenius activation energy approximately equal to the $\Delta v = 1$ vibrational spacing in NO. This behavior has again been interpreted as characteristic of strong coupling between NO and the metallic surface, whereby electron−hole pair formation in the metal couples efficiently with single-quantum excitation in the scattered NO molecules. Such a thermally assisted vibrational excitation mechanism has now become relatively well established for NO scattering from hot metal single-crystal surfaces, with the apportioning between adiabatic and nonadiabatic channels in principle extracted from temperature and incident energy dependence of the vibrational scattering event.[11,13] The feasibility and efficiency of such a vibrational up-pumping process become less clear, however, when the crystalline metal undergoes a phase transition from a single-crystal solid to hot molten liquid, due to dramatic changes in the gas−metal interface, the phonon spectrum, and density of states in the metal. Indeed, with the exception of recent studies of NO scattering from molten Au at extremely hot temperatures (T_{melt} = 1453 K), vibrational excitation in the scattered molecular species has proven quite elusive.[22] As one example of specific relevance, previous NO scattering from molten Ga at slightly cooler temperatures yielded only negligibly small vibrationally excited NO($v = 1$) signals below the detection limit.[23] This makes the issue of vibrational excitation efficiency for molecular projectiles in collisions with the gas−molten metal vs gas−single metal crystal interfaces therefore an interesting and open question for exploration.

The experiments herein describe first quantum-state-resolved NO scattering studies from hot molten gallium (Ga) at T_S = 600−1000 K, complementing and greatly extending the previous studies of NO + Ga(l) scattering up to 600 K.[23] Of particular interest, this paper presents first quantum-state results on vibrational excitation of scattered NO from the gas−molten Ga metal interface. Specifically, we have systematically investigated NO scattering dynamics from hot molten Ga surfaces as a function of (i) collision energy and (ii) surface temperature. These studies explore electronically nonadiabatic dynamics at the gas−metal interface with Ga(l) surface temperatures up to T_S = 1000 K, which is considerably hotter than previously accessible for these systems.[23−25] These experiments show first results of vibrationally excited NO($v > 0$) resulting from collisions with molten Ga surfaces, as well as experimental and theoretical evidence consistent with nonadiabatic energy transfer between electron−hole pairs in the liquid metal with the NO vibrational degree of freedom. Such electronically nonadiabatic behavior has been well studied for NO + single-crystal metal surfaces (e.g., NO + Au(111)),[11,13] but heretofore has not been possible to observe at the NO + molten Ga interface.

The organization of this paper is as follows. In Section II, we provide a brief description of the experimental setup, in particular focusing on modifications to the apparatus that permit scattering access to these higher molten Ga temperatures. This is followed by presentation of results in Section III, which report and analyze the final NO quantum-state distributions in rotational, vibrational, and electronic degrees of freedom, followed by a discussion of these distributions in Section IV. In Section IV, we also provide high-level MOLPRO complete active space self-consistent field (CASSCF)/AVnZ (n = 3, 4) calculations for the smallest metal cluster Ga−NO species,[26] which yield strong theoretical support for the presence of Ga to NO charge transfer as a function of the Ga−NO displacement coordinate. The paper concludes with a summary of results and directions for future exploration in Section V.

II. METHODS

The gas−liquid scattering apparatus has been described in detail previously.[23,27] Here, we provide a brief description of the setup while highlighting experimental changes made to the heating system that have enabled study of molten metals up to T_S = 1000 K and beyond. Simply summarized, supersonically cooled NO($^2\Pi_{1/2}$, $J = 0.5$) is scattered from freshly sputtered molten Ga(l) surfaces with quantum-state-resolved detection of the final NO, specifically, a molecular beam of NO rotationally and electronically cooled to the ground $^2\Pi_{1/2}$ spin−orbit state and $T_{rot} \sim 1$ K, with the NO seeded in either Ne or H_2 (1:99 ratio) buffer gas diluent to yield incident collision energies of 2.0(7) or 20(2) kcal/mol (0.087(30) and 0.87(9) eV), respectively. The molecular beam then passes through a 3 mm skimmer, creating a collimated beam striking the liquid surface at a 45° angle. This reduces the angular spread (1° HWHM) in the beam to ensure incident NO collisions with a suitably small footprint in the center of molten Ga, as well as overlap with the region cleaned by Ar^+ sputtering. The molten metal and scattering apparatus reside in a 90 L stainless-steel vacuum chamber pumped with a 1500 L/s turbomolecular pump, which maintains a $\sim 2 \times 10^{-8}$ Torr base pressure. The molten Ga reservoir is 3.8 cm × 1.3 cm, which is larger than the 0.8 cm × 1.1 cm spot size of the incident beam hitting the surface. The Even-Lavie valve pulses provide sufficient temporal resolution (<80 μs) to ensure probing only NO scattering from the metal surface under single-collision conditions. Specifically, the valve-laser time delay can be adjusted to monitor the NO molecule beam in the temporal domain, prior to, during, and after the pulse. This tells us unambiguously that the laser-induced fluorescence (LIF) signals are dominated by prompt single-collision NO scattering from the molten metal surface. Furthermore, signals immediately prior to the valve opening indicate that any trace amounts of background NO in the chamber due to finite pump-out time of the last gas pulse are negligible. In addition, spectral scans over the incident beam (see Figure S1) indicate extremely cold rotational temperatures on the order of 1−2 K, with a population ratio $<6.6 \times 10^{-4}$ between the spin−orbit excited and ground-state manifold and populations for $J > 4.5$ in the ground spin−orbit state below our current LIF sensitivity limits. Of particular relevance, the combination of extreme cooling and tight spatial filtering of the LIF means that rotationally thermal and hyperthermal components for both

https://dx.doi.org/10.1021/acs.jpcc.0c07861
J. Phys. Chem. C 2021, 125, 341−353

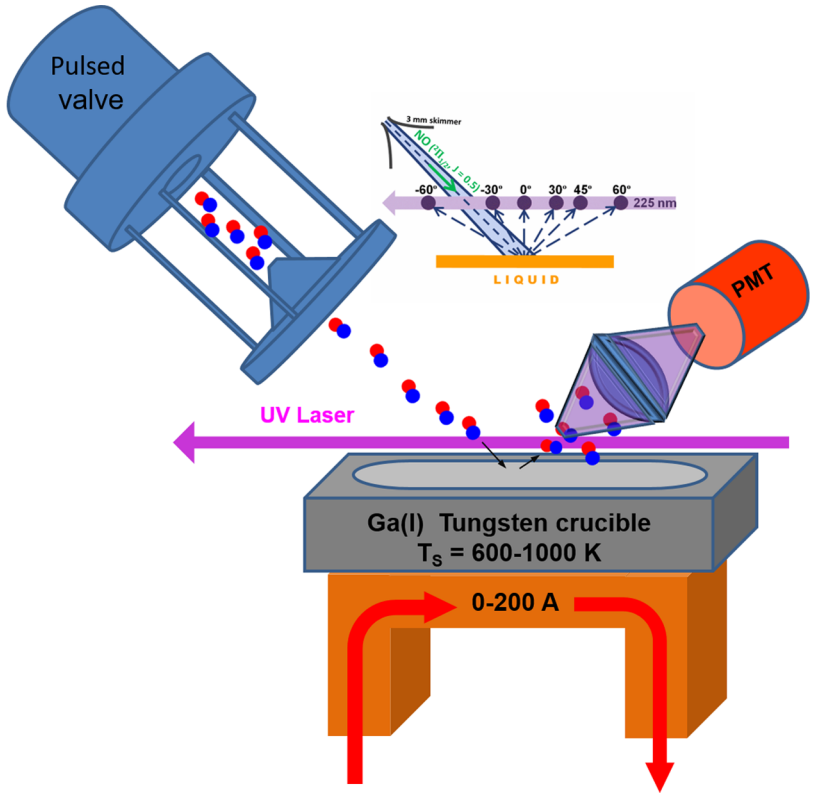

Figure 1. Apparatus for scattering at the gas−molten metal interface. Supersonically cooled NO ($^2\Pi_{1/2}$, $J = 1/2$) is scattered from molten Ga(l), which sits in a resistively heated tungsten crucible and can be heated up to $T_S = 600-1000$ K. Scattered NO molecules are detected with quantum-state resolution via LIF on the $A^2\Sigma^+(v' = 0) \leftarrow X^2\Pi(v'' = 0, 1)$ rovibronic sub-bands. The LIF is detected on a photomultiplier tube (PMT) with 1:1 imaging and spatial filtering capabilities to restrict the probe region and eliminate any residual contributions from the incident beam (see inset for a planar cross section of the detection geometries).

ground and spin−orbit excited NO($v = 0$) distributions arise solely from single-collision scattering events at the gas−molten Ga interface.

The essentials of heating the gas−molten metal interface are similar to previous studies with molten Au,[22] which required access to even higher temperatures ($T_S \approx 1500$ K). Ga metal sits in a tungsten crucible with an alumina coating along the edge to prevent wetting (S21-AO-W, R.D. Mathis). This, in turn, is resistively heated by a 4 kW power supply (LV400, R.D. Mathis), connected by a series of braided cables, solid feedthroughs, and solid Cu bars of sufficiently low electrical resistivity to minimize heating losses and maximize the power delivered to the tungsten boat. (Note: commercial names identified herein are for information only and do not indicate product support.) By way of a benchmark, it requires ∼300 W (207 Å at 1.45 V) to heat the 7 mΩ crucible to a temperature of 1400 K, for which the steady-state thermal losses are largely dominated by blackbody radiation ($\propto T_S^4$) from the hot molten metal surface.

The scattering apparatus and heating system are shown schematically in Figure 1. The Ga (99.9999%, Acros Organics) molten metal surface is cleaned by Ar^+ sputtering at 2 kV for several hours while heating the surface, with an additional 30 min of Ar^+ sputtering immediately prior to any spectral data scan. This sputtering procedure has been shown in previous inelastic collision studies[23] of NO from molten Ga(l) at lower temperatures (300−600 K) to yield reproducible changes in the NO LIF signal levels, which we attribute to scattering from a relatively clean metal surface into the pinhole filtered LIF detection volume. After this initial cleaning/heating period of several hours, the LIF spectra on the inelastically scattered NO remain stable over the time scale of the experimental data collection. The temperature is measured by a type K thermocouple contacted to the bottom of the tungsten boat, which has in turn been calibrated over different temperature ranges against measurements from (i) optical pyrometry ($T_S = 800-1200$ K) and (ii) a thermocouple submerged in the liquid Ga reservoir ($T_S = 300-850$ K). The upper temperature limit for these studies ($T_S = 1000$ K) is experimentally constrained by Ga vapor pressure.[28] Operation at $T_S = 600-1000$ K ensures that the sample is considerably above the melting point ($T_{melt} = 295$ K), but also cool enough to maintain sufficiently low vapor pressures ($P_{vap} < 10$ μTorr) above the liquid metal surface, ensuring long mean free path lengths ($\lambda \gg 1$ m) and thus single-collision conditions for NO molecular scattering prior to detection.[28,29]

Scattered NO molecules are detected with quantum-state resolution via laser-induced fluorescence (LIF) on the γ band, $A^2\Sigma^+(v = 0) \leftarrow X^2\Pi(v = 0, 1, 2)$. A pulsed UV light source (223−246 nm) is produced from the tripled output of a YAG pumped dye laser operating with LDS698 dye. The laser beam passes 1.6 cm above the liquid surface and in the plane of specular scattering with the laser polarization parallel to surface normal. The fluorescence of scattered molecules is imaged onto a photomultiplier tube (PMT), restricted to view only a ≈13 mm^3 volume along the laser path with a 1:1 confocal imaging setup and a 4 mm mask immediately in front of the PMT. This results in detection of scattered molecules isolated to near the specular angle $\theta_s = 45(6)°$. For the present hot Ga experiments, a cone is placed in front of the imaging lens to

https://dx.doi.org/10.1021/acs.jpcc.0c07861
J. Phys. Chem. C 2021, 125, 341−353

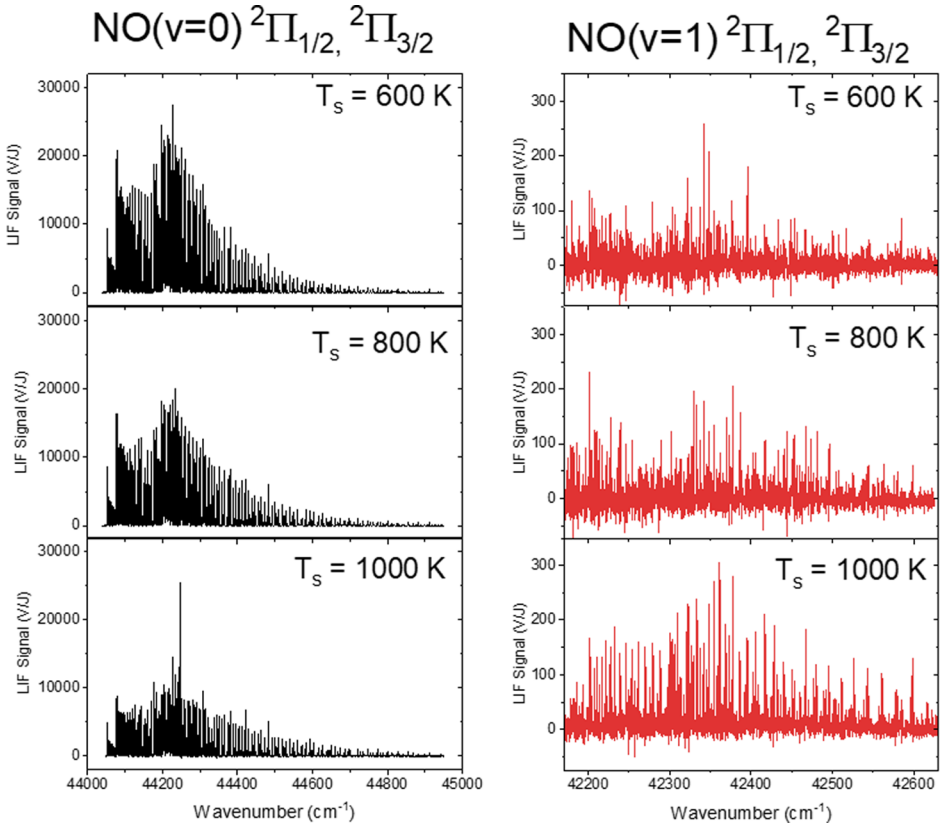

Figure 2. Sample spectra of NO(v'' = 0, 1; J; $^2\Pi_{1/2}$, $^2\Pi_{3/2}$) scattered at E_{inc} = 20(2) kcal/mol from Ga(l) as a function of molten metal temperature, detected via $A^2\Sigma^+(v' = 0) \leftarrow X^2\Pi(v'' = 0, 1)$ laser-induced fluorescence (LIF) arising from rovibronically resolved excitation out of NO in both (i) v = 0 (left panel) and v = 1(right panel) and (ii) lower ($^2\Pi_{1/2}$) and upper ($^2\Pi_{3/2}$) spin−orbit states. The raw data shown in figure represent half of the complete set of temperatures explored, with the results and trends for the remaining temperatures qualitatively consistent with the data actually presented.

block direct line of sight travel from the liquid surface. This cone allows all photons that originate in the detection volume to be collected by the PMT while preventing deposition of Ga on the lenses interfering with LIF detection efficiency over time. UV bandpass filters sit in front of the PMT to block incident laser light while maximizing the fluorescence gathered. Each vibronic band is detected in a different wavelength range, which in turn requires a different UV filter to block scattered light photons from the incident laser excitation: for NO(v = 0) (Thorlabs, UG5), NO(v = 1) (Asahi Spectra, XUV0325), and NO(v = 2) (Thorlabs, UG11), with comparisons of populations between the NO(v) vibrational states carefully corrected for the fluorescence transmission spectra of these filters. The PMT signal is integrated for 200 ns at the peak of the scattered NO signal in time and normalized to the laser power on a pulse-by-pulse basis.

III. RESULTS AND ANALYSIS

Sample LIF spectra for scattered NO(v = 0) and NO(v = 1) are displayed in Figure 2, where the fluorescence is generated and measured on the $A^2\Sigma^+(v' = 0) \leftarrow X^2\Pi(v'' = 0, 1)$ sub-band transition. The data are obtained at <1 μJ laser pulse energies and tested to ensure operation in the unsaturated linear regime, while the use of a common upper vibrational state $A^2\Sigma^+$NO($v' = 0$) eliminates the need for Franck−Condon/bandpass filter corrections in the fluorescence. The LIF spectra are then fit to a spectral model based on LIFBase rovibronic line strengths and excitation frequencies for NO detection, with methods tested and described in previous work from this laboratory.[23,30] In short, the analysis fits directly to a Gaussian model of spectral line shapes, floating a common laser limited transition line width ($\Delta\nu$ = 0.4 cm^{-1}), overall scaling factor, and small instrumental offset, but otherwise makes no assumption other than isotropic m_J distributions in the NO scattered flux. The reliability and reproducibility of this data fitting procedure have been quantitatively confirmed by least-squares fits to rotational/spin−orbit distributions of 1 × 10^{-6} Torr NO samples thermalized in the vacuum chamber, which recapitulate the correct room-temperature conditions to within a ±5 K experimental uncertainty.

The data in Figure 2 represent sample LIF spectral data for high collision energy NO (E_{inc} = 20 kcal/mol) scattering from liquid Ga surface for a series of three temperatures between 600 and 1000 K. By virtue of the constrained 1:1 imaging lens geometry, only NO molecules scattered in plane and in the forward specular direction are detected, with $\theta_{inc} \approx \theta_s \approx 45°$. Due to the large ground-state vibrational energy spacing ($\Delta E \approx 1876$ cm^{-1}) in NO, little to no vibrational cooling occurs in the pinhole supersonic expansion. However, also due to this large spacing, the stagnation region starts out with a negligibly small (<0.01%) thermal population of NO(v = 1) in the incident molecular beam. As a result, all NO(v = 1) species detected in the scattered flux necessarily arise from vibrational excitation via collisions at the gas−molten metal interface. Of particular relevance, the substantial energy transfer that we observe into both electronic (spin−orbit) and vibrational

https://dx.doi.org/10.1021/acs.jpcc.0c07861
J. Phys. C 2021, 125, 341−353

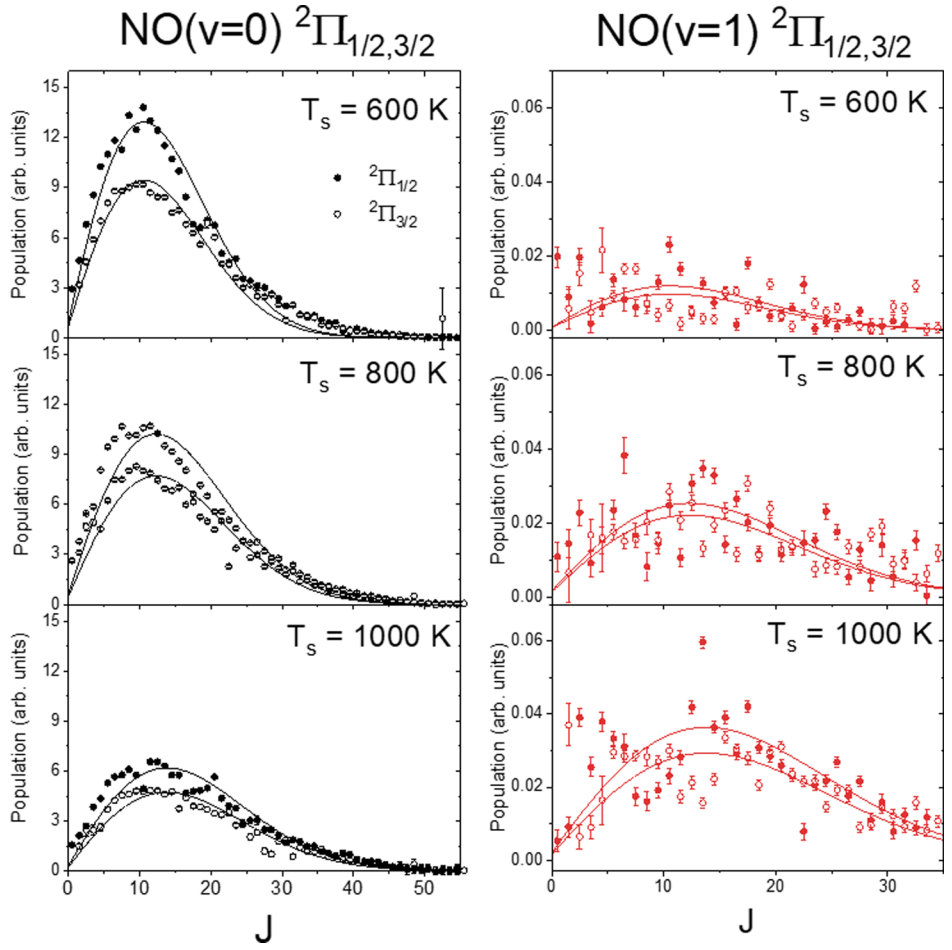

Figure 3. Rovibronic populations of ground state (left panels) and vibrationally excited state (right panels) scattered at E_{inc} = 20(2) kcal/mol from hot liquid Ga(l) as a function of temperature (T_S) at the gas−molten metal interface. Note that the solid lines in the plots at each temperature represent the predicted Boltzmann distribution at T_S.

degrees of freedom suggests the presence of nonadiabatic, charge-transfer dynamics occurring at the NO−Ga metal interface, as first proposed by Rettner et al.[1,41,4] Wodtke, Tully, and co-workers,[31−33] and that we briefly explore in Section V with preliminary ab initio calculations at the CASSCF/PV*n*Z (n = 3, 4) level.

For the moment, we consider a broad overview (see Figure 2) of the NO rovibronic distributions scattered at E_{inc} = 20 kcal/mol from molten Ga(l), obtained from averaging results from three replicate scans at each collision energy and surface temperature in the NO(v = 0, 1) spectral regions. The spectral data obtained at E_{inc} = 20 kcal/mol have been subjected to the least-squares fitting procedure described above, with the resulting rotational populations for ground spin−orbit ($^2\Pi_{1/2}$) and spin−orbit excited ($^2\Pi_{3/2}$) NO(v = 0) displayed in Figure 3 at each of three representative Ga(l) temperatures. It is important to stress that the incident NO starts in a nearly pure initial quantum state (i.e., NO $^2\Pi_{1/2}(v = 0, J = 1/2)$) with $<6.6 \times 10^{-4}$ population fraction in the excited $^2\Pi_{3/2}$ spin−orbit state manifold, as directly confirmed by LIF spectra of the initial beam (see Figure S1). Thus, both the spectra in Figure 2 and population plots in Figure 3 immediately showcase the presence of substantial energy transfer into excited rotational (J = 0.5−50.5), electronic spin−orbit ($^2\Pi_{3/2} \leftarrow {}^2\Pi_{1/2}$), and vibrational ($v = 1 \leftarrow 0$) states by collisions with the hot molten Ga surface. Though translation to rotational excitation might be expected for such collisions with a hot liquid surface, the origin of[2,3,5,34] facile excitation into both spin−orbit and vibrational degrees of freedom is less obvious. As will be discussed later in Sections III and IV, this exhibits many signatures for contributions from nonadiabatic dynamics at the gas−molten metal interface.

III.I. NO + Ga(l) Scattering: NO(v = 0) Rotational State Distributions. First, we examine the rovibronic distributions for NO(v = 0) scattered from molten Ga(l) into the vibrationally elastic channel. For more quantitative insight, we present sample Boltzmann plots in Figure 4a of ln[population(J)/(2J + 1)] vs internal rotational energy, focusing on the data subset for the spin−orbit excited $^2\Pi_{3/2}$ NO(v = 0; J) at E_{inc} = 2.0(7) and 20(2) kcal/mol and obtained for a fixed T_S = 873 K surface temperature. First of all, the semilogarithmic plots for the ground vibrational state rotational distributions (NO(v = 0), upper panel) exhibit a clear break into two additive linear components, which can be well fit to a "dual-temperature" double-exponential model characterized by T_{low} and T_{high}. It is important to emphasize that high levels of 1:1 imaging/spatial filtering in the LIF detection have been implemented to eliminate contributions of incident cold beam contamination to the populations extracted. This behavior would at first seem entirely consistent with "bifurcation" into trapping desorption (TD) and impulsive scattering (IS) pathways, which have been routinely identified

https://dx.doi.org/10.1021/acs.jpcc.0c07861
J. Phys. Chem. C 2021, 125, 341−353

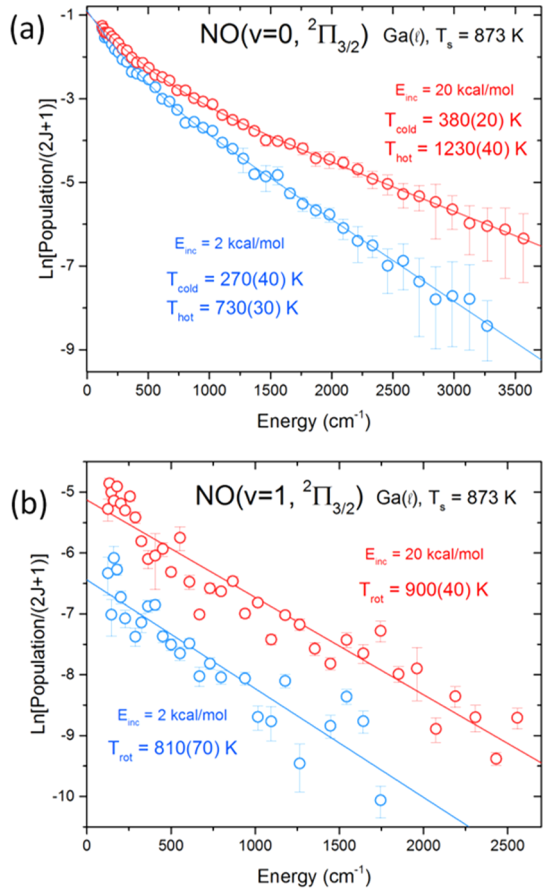

Figure 4. Boltzmann rotational distributions for NO scattered from Ga (T_S = 873(30) K) at both low (E_{inc} = 2.0(7) kcal/mol) and high (E_{inc} = 20(2) kcal/mol) collision energies. (a) Dual-temperature fits to NO(v = 0) rotational distributions and (b) single-temperature fits to vibrationally excited NO(v = 1), with $T_{rot} \approx T_S$ at both low and high collision energies within experimental uncertainties. The data all reflect nonadiabatic collisional excitation into the excited spin−orbit manifold ($^2\Pi_{3/2}$), which is completely unpopulated (down by >200-fold) in the incident beam due to supersonic cooling into a nearly pure NO(v = 0, n = 0, $^2\Pi_{1/2}$) quantum state. The data shown in figure in Figure 2 reflect 2/3 of the complete set of temperatures explored, with the results and all quantum-state-dependent trends for the remaining temperatures qualitatively consistent with the data presented.

in gas−liquid scattering studies via time-of-flight analysis of translations,[24,25] as well as for internal rotational degrees of freedom in quantum-state-resolved studies.[22,27,35−39] In particular, the lower temperature TD component in such studies often (but not always) reflects complete equilibration with the surface, with the higher temperature IS component responsible for capturing any dynamical (nonequilibrium) contributions to the scattering event. In the context of this standard TD/IS model, one might anticipate the lower temperature to match the surface ($T_{low} \approx T_S \approx$ 873 K), with a second "temperature" component hotter than the surface ($T_{high} > T_S$) and increasing with incident energy. Furthermore, for lower, less hyperthermal collision energies, one might expect a more complete equilibration to T_S and a corresponding increase in fractional branching into the TD channel. Interestingly, however, these predictions are clearly not what are observed.

Instead, dual-temperature least-squares fits of the NO(v = 0) data at low incident energy (E_{inc} = 2.0(7) kcal/mol) yield T_{cold} = 270(40) K and T_{hot} = 730(30) K, with T_{cold} 3-fold lower than T_S = 873 K and in clear disagreement with the above TD/IS model predictions. Furthermore, although the fits to the higher energy component do predict much higher T_{hot} values, this also appears to be completely uncorrelated with T_S. At the higher collision energy (E_{inc} = 20(2) kcal/mol), for example, the two temperature fits yield T_{cold} = 380(20) K and T_{hot} = 1230(40) K, which, although indeed reflecting the expected increase in T_{hot} with incident energy, still offers no evidence for a TD component remotely in equilibrium with the 873 K surface temperature. Most fundamentally, the standard TD/IS model cannot predict TD rotational distributions colder than the surface, the effects of which are clearly evident in the current data. We note that distributions out of equilibrium with T_S are not uncommon for desorption of NO from single-crystal Ag(111) and Au(111), which have been interpreted in terms of barriers along the desorption coordinate, detailed balance arguments, and nonunity sticking coefficients for the corresponding incoming flux.[40−43] These data raise important questions about the validity and applicability of standard TD/IS models for vibrationally inelastic gas scattering of NO from hot molten Ga, a point to which we will return later in Section IV. Specifically, the current data are consistent with a high rotational state deficit in the TD flux component, which, from detailed balance considerations, would be consistent with a reduced sticking coefficient for high rotational states in the reverse adsorption event.

III.II. NO + Ga(l) Scattering: NO(v = 1) Rotational State Distributions. For rovibronic excitation into the vibrationally excited NO(v = 1) channel (see Figure 4b), the collisional dynamics differ qualitatively. The greater scatter in these Boltzmann plots relative to the NO(v = 0) data (Figure 4a) is to be expected; this arises from the 50-fold lower population in NO(v = 1) ([v = 1]/[v = 0] = 0.019) and justifies only characterization by a single rotational temperature, T_{rot}. Interestingly, the fits now predict equivalent rotational temperatures (within experimental uncertainty) at both high and low collision energies. Specifically, we find T_{rot} = 900(40) K at high E_{inc} = 20 kcal/mol and T_{rot} = 810(70) K at low E_{inc} = 2 kcal/mol, with both temperatures now in much-improved agreement (within experimental uncertainty) with T_S = 873 K. This greater degree of similarity in rotational temperature observed for the NO(v = 1) vs NO(v = 0) manifolds is frankly surprising, yet dynamically interesting. One plausible suggestion is that vibrational excitation preferentially reflects results from more close collisions with the gas−molten metal interface, which offers a greater time for equilibration of the internal rotational degrees of freedom. It is important in this regard to note that the formation of excited NO(v = 1) is already evident at only E_{inc} = 2.0(5) kcal/mol, for which the incident collision energy alone would be insufficient (ΔE_{vib} = 1876 cm^{-1} = 5.36 kcal/mol) to excite NO(v = 1) without additional energy contributions from the molten Ga(l). While excitation from phonon modes in hot single-crystal metals could in principle serve as the energy source for these vibrational populations,[44] it is quite unlikely in the present case, as a sufficiently high-order multiphonon process ($n_{phonon} \approx T_{vib}/T_{Debye} \approx 10$ at T = 1000 K) would require interactions much longer than the surface scattering time (<few ps) to excite such a large nonresonant vibrational energy gap. Instead, such weak dependence of vibrational on collision energy is

https://dx.doi.org/10.1021/acs.jpcc.0c07861
J. Phys. Chem. C 2021, 125, 341−353

more consistent with a resonant excitation process dominated by the thermal population of electron−hole pair states in the hot metal, as clearly identified for NO + Au(111) by the experimental/theoretical work of Rettner et al. and Wodtke, Tully, and co-workers.[1,4,31,33] We will make further confirmation of such a thermally promoted electron−hole pair mechanism by temperature-dependent studies of the vibrational excitation efficiency, as presented in Section IV.I.

III.III. Rotational/Spin−Orbit Excitation: Dependence on Molten Ga(l) Temperature. We next return to the NO(v = 0,1) scattering data in Figure 4 at high collision energy (E_{inc} = 20 kcal/mol), but now focusing on the level of rotational and electronic spin−orbit excitation as a function of the molten Ga temperature (T_S). Though the two spin−orbit manifolds in NO are not perfectly uncoupled, we have chosen in the interest of simplicity to characterize this degree of freedom by an effective temperature, T_{elec}. This temperature estimate is obtained by summing up all rotational populations in the ground ($^2\Pi_{1/2}$) and excited ($^2\Pi_{3/2}$) spin−orbit states for a given NO(v), and extraction from the simple Boltzmann expression

$$P(^2\Pi_{3/2})/P(^2\Pi_{1/2}) = \exp(-\Delta E_{SO}/kT_{elec}) \quad (1)$$

where $\Delta E_{SO} \approx 120$ cm^{-1} reflects the spin−orbit splitting of the two manifolds at low rotational energy (Hund's case a).[45] Comparable estimation of an effective temperature for the rotational degrees of freedom is complicated by curvature in the Boltzmann plots, which we simply finesse by assuming the correspondence principle classical limit of $T_{rot} \approx <E_{rot}>/k_B$. Again, the results for both rotational and spin−orbit effective temperatures are plotted in Figure 5 as a function of surface temperature, T_S, for elastic and inelastic scattering into NO(v = 0) and NO(v = 1) channels, respectively, and reveal several interesting trends.

First of all, despite such a crude treatment, the rotational temperatures indicate a remarkably smooth progression for both NO(v = 0) and NO(v = 1) data. In particular, the effective rotational temperature data for NO(v = 1) (open circles) in Figure 5 fall quite close to the $T_{eff} = T_S$ solid line, therefore suggesting closer thermal equilibration of these average NO energies with molten Ga(l). Indeed, the positive deviations away from the $T_{eff} = T_S$ equilibration line occur systematically toward the lower values of T_S, which may reflect the fact that hyperthermal E_{inc} = 20 kcal/mol conditions represent more than a perturbative contribution to the total energy. Finally, this trend in agreement between effective rotational and surface temperatures is also quite good (and arguably even improved at low T_S) for scattering into the vibrationally excited channel NO(v = 1) (Figure 5). This is consistent with the NO(v = 1) scattering data in Figure 4b, where the single exponential temperature fits are already within the experimental uncertainty of T_S. More work would be necessary to confirm this, but one speculation might be that energy flow from thermally populated electron−hole pairs in molten Ga into the NO vibrational coordinate is enhanced by longer gas−surface interaction times, thus achieving a closer rotational equilibration between the surface and the molecular projectile.

The corresponding effective spin−orbit temperatures (T_{elec}) for NO(v = 0) also show a similar increasing trend with surface temperature (see Figure 5, upper panel), although now distinctly lower than the $T_{eff} = T_S$ solid line representing full equilibration. It is important to remember that the incident

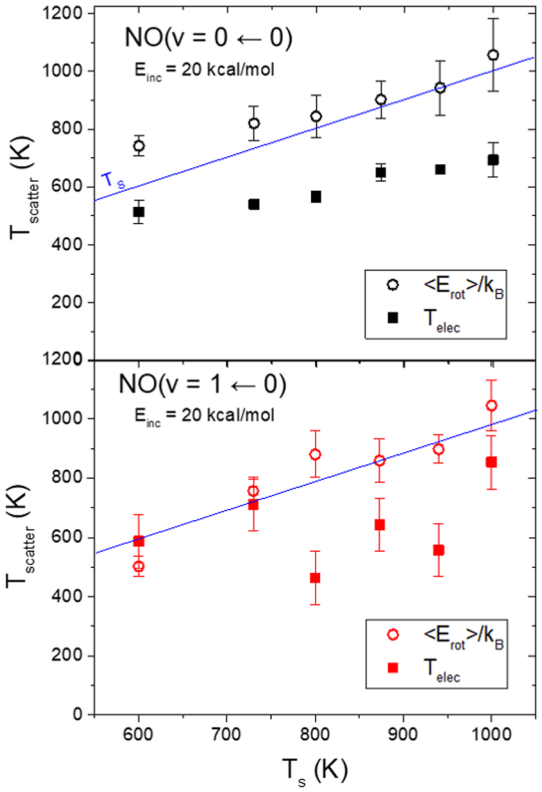

Figure 5. Effective rotational ($<E_{rot}>/k_B$) and electronic (T_{elec}) temperatures of vibrational ground (v = 0) and first excited (v = 1) states, formed by scattering NO from hot molten Ga(l) as a function of surface temperature.

beam contains NO(v = 0) purely in the ground $^2\Pi_{1/2}$ spin−orbit state and that any collision excitation into the excited state $^2\Pi_{3/2} \leftarrow {}^2\Pi_{1/2}$ therefore represents a nonadiabatic, surface hopping event. With such nonadiabatic effects providing additional dynamical barriers to exchange between spin−orbit states, it is therefore perhaps not surprising to see deviations below the surface temperature ($T_{elec} < T_S$). There is clearly a residual sensitivity to surface temperature (with a local slope $dT_{elec}/dT_S \approx 0.5$), which could reflect a shortening of residence times on the surface with increasing temperature. Finally, although the corresponding data (Figure 5, lower panel) for the vibrationally inelastic NO(v = 1) channel has substantial additional scatter due to a 50-fold reduction in signal, it is still visually consistent with the more smoothly increasing trend demonstrated for NO(v = 0).

IV. DISCUSSION

In previous molecular scattering experiments at the gas−liquid interface, a two-temperature fit has often been used to describe a colder, thermal desorption (TD) scattering pathway, with rotational temperatures near the surface temperature, and a rotationally hotter, impulsive scattering (IS) channel. At lower surface temperatures, this simple and physically motivated model has been extremely useful in characterizing translational and rotational distributions. However, at these higher surface temperatures (T_S = 873 K), while the rotational distributions indeed well fit a two-temperature model, the rotational temperatures need not necessarily lend themselves to a simple TD/IS scattering picture. The reason for this may be a dynamical combination of high surface temperatures and short

https://dx.doi.org/10.1021/acs.jpcc.0c07861
J. Phys. Chem. C 2021, 125, 341−353

interaction times. In particular, the incident NO beam is initially in an extremely cold ($T_{rot} \approx 1-2$ K) distribution of internal rotational and spin−orbit states, colliding abruptly with the molten Ga surface. If the interaction time with the liquid surface is sufficiently short, one might expect only limited thermal energy transfer to and thus a truncated "warming" of the initially cold molecule prior to escape.[35] If this were true, the colder rotational temperatures derived from these fits need not be associated with an equilibrium process at all, but rather might reflect a new nonequilibrium "IS" channel for time-limited interaction of NO molecules with the molten metal, with NO scattering away with subthermal rotational excitation.[35] From a detailed balance perspective, this would imply a quantum-state dependence on the sticking coefficients, with a lower sticking probability for higher rotational states in the reverse adsorption process.

IV.I. Vibrational Excitation of NO(v): Dependence on Molten Ga(l) Temperature. As one particular dynamical theme of this work, we consider how the temperature of the molten Ga interface influences the scattering NO(v) vibrational degree of freedom. In the interest of completeness, we first searched for NO($v = 2$) on the $X^2\Pi(v'' = 2) \leftarrow A^2\Sigma^+(v' = 0)$ sub-band transition. However, no peaks assignable to NO($v = 2$) were found in this region, with signal integration over the predicted spectral range permitting an estimated upper limit of $[v = 2]/[v = 0] \leq 1.5 \times 10^{-3}$. Thus, the LIF signals for NO($v = 2$) would be reduced from the NO($v = 0$) and NO($v = 1$) signals in Figure 2 by 670- and 12-fold, respectively, and thus visible only at the very highest vapor pressure-limited Ga(l) surface temperatures accessible in our apparatus. Thus, at our current LIF sensitivities, we only report data on NO($v = 0$) ground and NO($v = 1$) vibrationally excited states, with the latter populations reduced by 55-fold from the former at $T_S = 873$ K.

We can, nevertheless, still extract an effective vibrational temperature (T_{vib}) from such two-point data for NO scattered from Ga(l), simply by integrating over all rotational and spin−orbit populations within each $v = 0$, 1 vibrational manifold and utilizing the Boltzmann expression

$$P_{v=1}/P_{v=0} = \exp[-\Delta E_{vib}/(kT_{vib})] \quad (2)$$

where the vibrational energy spacing between NO($v = 0$) and NO($v = 1$) is $\Delta E_{vib} = 1876$ cm^{-1}. For example, the experimentally observed population ratio of $P_{v=1}/P_{v=0} = 0.019$ at $T_S = 873$ K corresponds to $T_{vib} = 708(35)$ K, which is closer to and yet still significantly cooler than the actual molten Ga surface. A more complete set of such vibrational temperature data as a function of T_S is presented in Figure 6, which again reveals a smoothly increasing trend, albeit with significant displacement below the solid line, representing full equilibration ($T_{vib} \approx T_S$) of the vibrational coordinate with the molten Ga(l) surface temperature.

IV.II. Arrhenius Vibrational Excitation of NO Scattered from Ga(l). To further probe the mechanism for NO excitation by collisions with a molten metal surface, we have explored vibrational, rotational, and spin−orbit excitation dynamics as a function of the liquid gallium surface temperature T_S. For the Boltzmann analysis data reported in Figure 4, LIF spectra containing all rotational and spin−orbit states populated within NO($v = 0$) and NO($v = 1$) were obtained at a single $T_S = 873$ K, from which we could extract the full Boltzmann rotational and spin−orbit distributions. This requires extensive scanning in triplicate above around

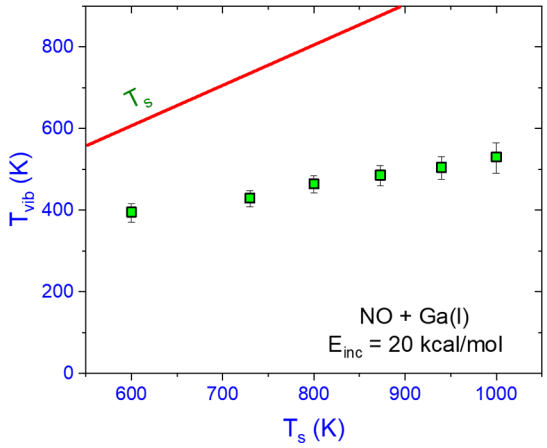

Figure 6. Dependence of scattered NO vibrational temperatures (T_{vib}) on the surface temperature of the molten Ga metal (T_S). The results reveal strongly nonequilibrium behavior (specifically $T_{vib} < T_S$) with a modest but clearly finite sensitivity to T_S.

1400 cm^{-1}, which is not practical to perform for a series of multiple surface temperatures. We can, however, speed up this process substantially by scanning over a more information-dense subset of the spectrum, thereby obtaining reliable estimates of these vibrational temperatures as a function of T_S, Specifically, the P_{12} band head proves to be the optimal choice and can be scanned relatively quickly from $J = 1.5-19.5$ for both $v = 0$ and 1, therefore yielding reliable vibrational state population ratios over an equivalent range of J. The vibrational temperatures extracted from these ratios are reported in Figure 6 over the full range of surface temperatures $T_S = 600-1000$ K. These data reveal a smooth increase in vibrational excitation efficiency with surface temperature, yet again with distinctly subthermal values ($T_{vib} < T_S$) and a reduced slope ($dT_{vib}/dT_S \approx 0.33$). It is worth emphasizing that such subthermal scattering behavior[46] is already in qualitatively good agreement with previous NO scattering results from solid single-crystal surfaces.[20]

However, we can take such a T_S-dependent analysis considerably further. In previous scattering experiments of NO from crystalline surfaces, an activated Arrhenius surface temperature dependence has been interpreted as characteristic evidence for nonadiabatic, electron−hole pair-mediated energy transfer between NO and metal surfaces.[1,13,18,21,47] To further investigate this possibility, the vibrational excitation probability ratio, $P_v = [v = 1]/[v = 0]$, is expressed as an Arrhenius-type equation[29]

$$P_v = A \exp[-E_a/kT_s] \quad (3)$$

where A is the Arrhenius prefactor and E_a is the activation energy. The data are plotted in Figure 7, which reveals highly linear behavior in $\ln(P_v)$ vs $1/T$, in excellent agreement with predictions of eq 3. Of particular interest, the slope of this plot corresponds to an activation energy of $E_a = 1850(200)$ cm^{-1}, which is in quantitative agreement with the $v = 1 \leftarrow 0$ vibrational energy spacing in NO ($\Delta E_{vib} = 1876$ cm^{-1}).[48] Based on models developed from previous studies,[12,13] this would be consistent with strong vibronic coupling of NO with the molten metal, whereby thermal generation of an electron−hole pair state of energy ΔE_{vib} can resonantly excite NO($v = 1$) via NO($v = 0$) collisions at the liquid Ga surface. Wodtke, Tully, and co-workers have contributed extensively toward

https://dx.doi.org/10.1021/acs.jpcc.0c07861
J. Phys. Chem. C 2021, 125, 341−353

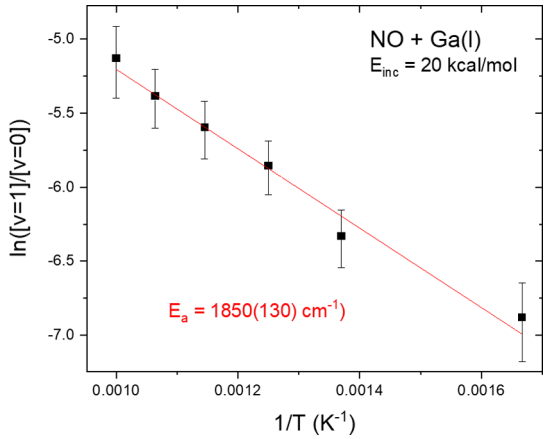

Figure 7. Activated Arrhenius analysis of the vibrational excitation probability for NO(v = 1 ← 0) scattering from liquid Ga(l) vs surface temperature. The blue line represents an Arrhenius fit with E_a = 1850(130) cm^{-1}, which is well within uncertainty of the NO vibrational energy spacing (1876 cm^{-1}). The intercept yields an Arrhenius prefactor (ln[A] = −2.5, A = 0.082(33)) less than unity, which, from the kinetic analysis of Matsiev et al.,[13] indicates that the collisional interaction time is insufficient to achieve full thermal equilibrium with the molten Ga surface. Interestingly, these A values are consistent with results previously observed for NO scattering from molten Au (A ≈ 0.12) but significantly smaller than values for NO scattering from Au(111). Of greatest relevance, this Arrhenius behavior is consistent with models for vibrational excitation of NO via resonant energy transfer from thermally generated electron−hole pairs.[1,5,9,11,13]

understanding these nonadiabatic, electron−hole pair-mediated collision dynamics occurring at NO + Au(111) surfaces.[5,9,11,13,31−33,49] Substantial evidence has been presented that suggests that vibrational relaxation of NO(v) at a metal surface is mediated by the formation of resonant electron−hole pairs in the single-crystal metal. Interpreted in the context of this earlier work, the present results represent additional quantum-state-resolved support for electron−hole pair-mediated vibrational excitation of NO(v) at the gas−molten metal interface.

As one well-known physical picture for such a vibronic coupling mechanism, the NO molecule approaches the surface on a one-dimensional (1D) NO ($^2\Pi$) + Ga(l) neutral potential surface, for which one must also consider the corresponding anion NO$^-$ ($^3\Sigma_g^+$) approaching a cationic Ga(l)$^+$ with a steep 1/R Coulombic potential. At some short distance (typically ∼ 1 Å), these two 1D surfaces cross, at which point the ground state of the system corresponds to NO$^-$ ($^3\Sigma_g^+$) + Ga(l)$^+$. Simply stated, charge transfer out of the highest energy orbitals near the Fermi level of the Ga metal "hops" onto the NO to form a transient NO$^-$ anion, strongly Coulombically stabilized by image charge redistribution in the conductive metal. As the transient NO$^-$ anion collides with and recoils from the surface, the anion can detach back to the metal and allow neutral NO to escape. Since both the N−O stretching potential and equilibrium geometry depend strongly on the charge state, this provides a simple, physically motivated vibronic coupling mechanism by which vibrational quanta can be generated (or lost) in the NO molecule.[31,33]

It is instructive to extend this Arrhenius analysis one step further to ask why such a resonant mechanism based on thermally generated electron−hole pairs (as demonstrated by Figure 7) does not predict the scattered NO(v) to be in perfect equilibrium with the hot Ga metal (as equally clearly not demonstrated by Figure 6). The short answer depends on the value of the Arrhenius A factor, which, for A ≈ 1, would immediately require T_{vib} ≈ T_S by equating the two expressions for P_v in eqs 2 and 3. In fact, this A factor is an order of magnitude lower than unity, as obtained by extrapolation of the Arrhenius fit in Figure 7 to zero (T = ∞), yielding ln[A] = −2.5(2) or A = 0.082(33). Intriguingly, this value of the Arrhenius prefactor for NO + molten Ga is nearly 5 times smaller than previously observed (A = 0.38) for NO(v = 1 ← 0) excitation in scattering from single-crystal Au(111).

To best interpret these results, we turn to the Fermi golden rule kinetic analysis of Matsiev et al., which yields remarkably simple analytical expressions characterizing Arrhenius behavior and Arrhenius prefactors for a nonadiabatic vibrational excitation of NO by thermally populated electron−hole pairs in Au(111).[13] In the context of this theory, the rate constants for vibrational excitation and de-excitation are given analytically by

$$k_{v v'}(T) = \alpha_{v v'} E_{v v'} / [\exp(E_{v v'}/kT_S) - 1] \quad (4)$$

where $E_{vv'}$ is the vibrational spacing, $\alpha_{vv'}$ = $(2\pi/\hbar)$ $\lambda_{vv'}{}^2$ $\rho^2(E_{vv'})$, $\lambda_{vv'}$ = |<v|H|v'>|, and $\rho(E_{vv'})$ is the density of states in the metal resonant with $E_{vv'}$. Note that in the low-temperature limit ($T \ll E_{vv'}/k \approx$ 2700 K), eq 4 naturally predicts thermally activated Arrhenius behavior with a slope = $-E_{vv'}/k$, as experimentally confirmed in Figure 6. Furthermore, from exact solution to this system of rate equations, the Arrhenius prefactor ($A = \alpha_{vv'} E_{vv'} t$) is predicted to scale linearly for short gas−interfacial interactions ($k_{vv'}\tau_{res} \ll 1$) and asymptotically saturate at 1.0 when the system has time to achieve full thermal equilibrium with the molten Ga surface. Based on the above kinetic analysis, the experimental observation of subunity Arrhenius prefactors immediately implies that thermal equilibrium is not achieved on the residence time scale of a single NO−molten Ga surface collision, and is furthermore lower by an additional 4−5-fold than for NO−Au(111) collisions (A = 0.38). Whether this reflects a difference in density of states ($\rho_{vv'}$), reduced vibronic coupling between NO and molten Ga ($\lambda_{vv'}$), or simply a shortened interaction time with the surface (τ_{res}) cannot be unambiguously determined from the current data set, though experiments that probe NO excitation further up the vibrational ladder to v = 2 ← 0 may prove more revealing. However, it is already interesting to note that reduced Arrhenius prefactors of order A ≈ 0.1 appear to be also consistent with measurements for NO scattering from molten Au at 1400 K, which, if one reasonably assumes Arrhenius behavior (i.e., slope = $-E_{vv'}/k$), predict A = 0.12(2).

IV.III. *Ab Initio* Support for Charge-Transfer Dynamics at the Gas−Molten Metal Interface. The above dynamical model for NO vibrational excitation suggests that we should be able to see evidence for such a charge transfer from sufficiently high-level ab initio Born−Oppenheimer calculations of NO approaching molten Ga(l)−NO. Although modeling NO in the vicinity of molten Ga(l) liquid is beyond the scope of any ab initio calculations we can perform at the present time, it is nevertheless interesting to start toward such a goal with ab initio calculations for van der Waals clusters of Ga$_n$−NO. Indeed, in this last section, we take this approximation to the ultimate limit and consider only the very first step on this journey, specifically, calculations of the very simplest metal cluster−NO adduct (n = 1), Ga−NO. Our hope is to gain first

https://dx.doi.org/10.1021/acs.jpcc.0c07861
J. Phys. C 2021, 125, 341−353

insights into the binding energy of NO with Ga as well as preliminary information on the nature of charge transfer in the Ga−N bond-formation process.

Ga−NO has a triplet ground state that dissociates asymptotically into Ga (^{2}P) and NO($^2\Pi$), each with 3- and 2-fold degeneracies, respectively. The presence of multiple low-lying electronic degeneracies makes this an intrinsically multireference problem near the dissociation limit, for which single-reference calculational methods such as Hartree−Fock and density functional theory (DFT) are known to perform poorly. Instead, we choose to pursue multiconfigurational self-consistent field (MCSCF) (i.e., state-averaged CASSCF) calculations available in the MOLPRO suite of ab initio code, which allows us to systematically optimize the orbital space with respect to all six of these asymptotically nearly degenerate states.[26,50]

For the linear NO approach toward Ga on the ground triplet surface, these 3 × 2 = 6 nearly degenerate electronic levels split into states of Σ^+ and Δ ($^3A_1$), Π ($^3B_1$), $^3\Pi$ ($^3B_2$), and Σ^- + Δ ($^3A_2$) symmetries, where the labels in parentheses refer to irreducible representations of the C_{2v} group. We therefore perform six-state-averaged, full-valence CASSCF calculations for these six electronic triplet states, with the lowest 10, 3, 3, 1 orbitals of A_1, B_1, B_2, A_2 orbital symmetries, respectively, optimized but constrained to be doubly occupied in the wave function, optimizing the NO bond length. We then use these optimized orbitals to perform a second CASSCF calculation focusing explicitly on the $^3\Sigma^-$ ground state, utilizing a natural bond orbital (NBO) analysis to evaluate the charge properties of the individual atoms. This process is then repeated by scanning the Ga−N bond distance from R_{GaN} = 4.0−1.7 Å in 0.1 Å steps, optimizing the NO bond length, and generating a 1D potential energy curve with the resulting CASSCF energies. Finally, we test for suitable levels of convergence by repeating this whole process for aug-cc-pVnZ (AVnZ) Dunning basis sets with n = 3, 4.[51,52] At the CASSCF/AVTZ level, the 1D potential for the ground $^3\Sigma^-$ state corresponds to a binding energy of D_e = 25.36 kcal/mol at R_{GaN} = 2.0 Å. Good convergence with respect to basis set size is indicated by the only very small changes ($|\Delta E|$ < 0.05 kcal/mol) in this value predicted from additional calculations at the higher CASSCF/AVQZ level.[53−55]

Of particular interest to the present study are the atomic charges predicted from natural bond orbital (NBO) analysis of these CASSCF wave functions, which have been plotted in Figure 8 as a function of R_{GaN} distance along the ground $^3\Sigma^-$ state potential surface. At large R_{GaN}, Ga is asymptotically neutral, with the NO exhibiting a modest partial electron transfer (0.19e) from N to O. As NO approaches Ga, however, the NBO analysis indicates a notably significant charge transfer from Ga to N, reaching values of +0.6e and −0.40e, respectively, at the equilibrium position. Such significant charge redistribution dynamics takes place between R_{Ga-N} = 2.0 and 2.5 Å and corresponds approximately to single electron transfer from Ga to N, strongly echoing the mechanism proposed by Tully and Wodtke for transient formation of a transient NO negative anion in proximity to a conducting Au(111) single-crystal surface.[31−33] We can provide additional support for this model by further analysis of the CASSCF wave functions as a function of R_{GaN} separation. Specifically, intramolecular electron flow isocontours have been calculated for Ga−NO near the equilibrium geometry, expressed in terms of the differential electron density, $\delta|\Psi|^2 \approx |\Psi(2.01\ \text{Å})|^2 - |\Psi(1.99\ \text{Å})|^2$, at R_{GaN}(eq) = 2.00 Å. A representative isocontour for this differential density in Ga−NO is plotted in Figure 9, where the electron flow from Ga to N is evidenced by a dominant increase in electron density (light blue) between the Ga and N, with concomitant depletion of density (light purple) from the Ga atom itself. Simply summarized, we see good agreement in these CASSCF ab initio calculations with the early model predictions of Tully, Wodtke, et al.[31,33]

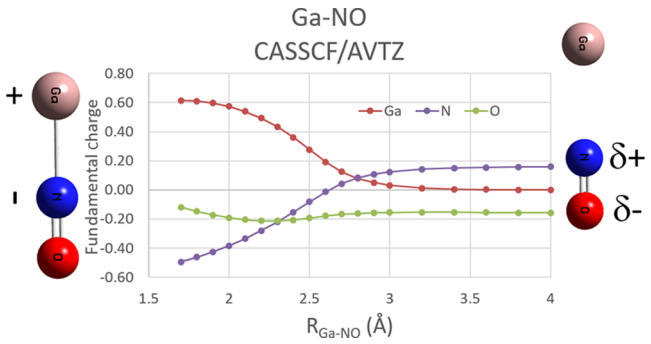

Figure 8. Atomic charge distributions in Ga−NO evaluated from natural bond orbital (NBO) analysis of the ground-state $^3\Sigma^-$ wave function obtained at the CASSCF/AVQZ level. The lowest 10 orbitals are constrained to be doubly occupied, and the CASSCF calculations are performed for the lowest six states ($A_2(\Sigma^-)$, $A_1(\Delta)(2x)$, $B_1(\Pi)$, $B_2(\Pi)$, $A_1(\Sigma^+)$) expected asymptotically for a $^2\Pi$ molecule (NO) plus a ^{2}P atom (Ga). Especially noteworthy is the dramatic charge redistribution occurring as a function of Ga−N bond distance, from a small dipole moment asymptotically (R_{Ga-N} > 4.0 Å) on N−O to a large dipole moment on Ga−N at the near-equilibrium geometry ($R_{Ga-N} \approx$ 2.0 Å). Although this is only for a single Ga atom, this establishes plausibility and provides preliminary support for the presence of short-range charge transfer and nonadiabatic surface hopping dynamics in collisions of NO at the molten Ga interface.

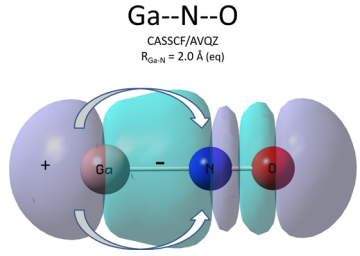

Figure 9. Sample contour plot of the differential electron density (0.00005 isoval) for ground-state ($^2\Sigma^-$) ab initio wave functions at the CASSCF/AVQZ level, evaluated at the equilibrium geometry between R_{Ga-N} = 2.01 and 1.99 Å and again providing strong evidence for significant charge transfer (0.6e^-) from the Ga to the N atom. Similar to the calculations in Figure 8, the lowest 10 orbitals are constrained to be doubly occupied, and the CASSCF calculations are performed for the lowest six states ($A_2(\Sigma^-)$, $A_1(\Delta)(2x)$, $B_1(\Pi)$, $B_2(\Pi)$, $A_1(\Sigma^+)$) expected asymptotically for a $^2\Pi$ molecule (NO) plus a ^{2}P atom (Ga).

In closing, we offer three parting comments. First of all, it is important to stress that a single Ga atom in Ga−NO will not recapitulate the charge-transfer and image charge properties of a full semi-infinite conducting Ga(l) surface. Nevertheless, the present ab initio results are certainly encouraging and provide supporting evidence for transient NO anion formation taking place at the gas−molten Ga(l) interface. This also suggests that it could be quite interesting to extend such ab initio efforts to more realistic Ga(l)−NO clusters, perhaps by a combination of

https://dx.doi.org/10.1021/acs.jpcc.0c07861
J. Phys. Chem. C 2021, 125, 341−353

high-level ab initio calculations[26,50,53−55] for a small local cluster Ga_n−NO (n = 1, 2, 3...) supplemented by embedding potential calculations for the surrounding molten metal.[56−58] Efforts toward such a broader treatment are currently in progress and will be presented elsewhere.

Second, although strong fractional charge transfer is clearly evidenced in Figure 8 between Ga and N with decreasing R_{GaN} bond length, it is equally strongly predicted from ab initio calculations for stretching/compression of the NO bond. This represents a clear mechanism for strong nonadiabatic vibronic coupling with the NO(v) vibrational coordinate.[5,16,34] This coupling can be anticipated to play a particularly significant role in the dynamics of vibrational excitation via resonant electron−hole pairs formed thermally in the hot metal, as well as the reverse process of nonadiabatic vibrational relaxation dynamics for NO(v) in collisions with single-crystal metal surfaces. Interestingly, this strong coupling between NO bond stretching and electron energy transfer between the metal atom and adsorbed NO molecule also predicts intense enhancement of vibrational IR activity in the NO stretch mode.

Finally, it is worth noting that NO in the incident beam is purely in the ground electronic state, whereas the scattered NO is experimentally found to have large contributions from both ground ($^2\Pi_{1/2}$) and excited ($^2\Pi_{3/2}$) spin−orbit excited states. For a Hund's case a molecule,[59] this represents a change in the total spin + electronic projection ($\Omega = |\Lambda + M_s|$) quantum number, requiring a low probability nonadiabatic surface hopping between the Ω = 1/2 and 3/2 potential surfaces. The possible formation of a transient NO^- anion at the gas−metal interface provides a simple physical mechanism for this to be an efficient process, as schematically shown in Figure 10. Specifically, molecular orbital theory predicts the highest occupied molecular orbital (HOMO) for NO to be a $2p\Pi_x^*$ or $2p\Pi_y^*$ antibonding orbital,[59] with the ground state $\Omega = |\Lambda + M_s| = 1/2$ arising from $\Lambda = -1$ and $M_s = 1/2$ spin−orbit coupling. By analogy with isoelectronic O_2, the ground-state configuration of the transient NO^- anion is $^3\Sigma^-$, corresponding to triplet coupled electrons (Λ = 0, M_s = 1) in the two degenerate $2p\Pi_{x,y}^*$ molecular orbitals. When the electron returns to Ga(l), it can be from either molecular orbital, which would provide a simple physical mechanism for generating asymptotically scattered NO in either the ground ($^2\Pi_{1/2}$) or excited ($^2\Pi_{3/2}$) spin−orbit state. Simply stated, the ability to swap orbital angular momentum components between $\Lambda = -1$ and 1 via the transient NO^- anion intermediate could provide an efficient mechanism for achieving a change in Ω without the need for any corresponding change in electron spin projection M_s.

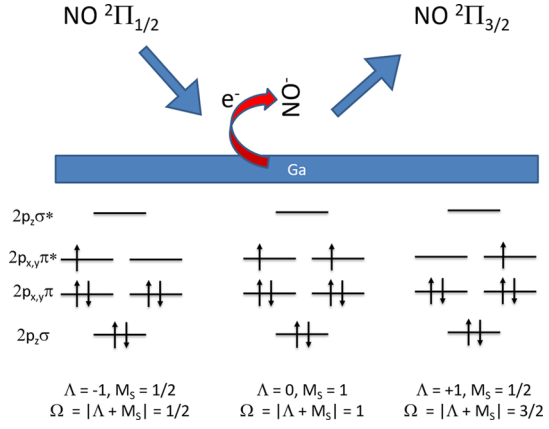

Figure 10. Simple picture for why transient electron transfer to form the transient NO^- anion in collisions at the gas−molten Ga metal interface provides a facile pathway for nonadiabatic changes in the spin−orbit state distribution. Specifically, the cooled NO ($^2\Pi_{1/2}$) spin−orbit state present in the supersonic expansion can transiently pick up an electron into the $2p_{x,y}$ π^* antibonding orbital to form NO^- ($^3\Sigma^-$) with total Λ = 0. Release of electron back to the metal from the Λ = +1 antibonding orbital yields asymptotic formation of the $^2\Pi_{3/2}$ spin−orbit state without any electron spin flip. This provides a very simple physical mechanism for facile nonadiabatic energy transfer between the $^2\Pi_{1/2}$ and $^2\Pi_{3/2}$ spin−orbit manifolds of NO in collisions at the molten Ga interface.

V. SUMMARY AND CONCLUSIONS

Quantum-state-resolved molecular beam scattering techniques have been utilized to investigate collision dynamics of NO at molten gallium surfaces. The results represent the first detection of vibrationally excited NO(v > 0) from collisions at the gas−molten Ga interface. Indeed, with the exception of recent NO + molten Au studies[22] at much higher temperatures (1400 K), this represents the only detection of vibrationally excited NO(v > 0) at a gas−molten metal interface. Additionally, the surface temperature dependence of these vibrational excitation probabilities exhibits a thermally activated, Arrhenius-like behavior. The activation energy (E_a = 1850(130) cm^{-1}) extracted from such an Arrhenius analysis is in excellent agreement with the 1896 cm^{-1} Δv = 1 spacing in NO, behavior that has been interpreted as strong evidence for vibrational excitation via thermal generation of resonant electron−hole pairs. Rovibronic distributions for the vibrationally elastic channel NO(v = 0) reveal dual-temperature behavior, with least-squares fits yielding temperatures out of equilibrium with the Ga(l) surface, as well as a relatively strong dependence on collision energy. By way of contrast, the rovibronic distributions in the inelastically vibrationally excited NO(v = 1), however, prove to be relatively insensitive to collision energy and reveal a single temperature in better agreement with T_S. Moreover, the rotational and spin−orbit distributions are remarkably similar for NO(v = 1) scattered from low and high collision energies for both Ga(l), suggesting that these internal NO modes are predominantly excited by thermal electron−hole pairs in the metal surface. These experimental results have stimulated first efforts at ab initio MOLPRO CASSCF/AVnZ (n = 3, 4) calculations on Ga−NO as the simplest model system, which reveal compelling evidence for charge transfer from Ga to the N atom as a function of R_{GaN}. Although more work will clearly be necessary to test these ideas further, the current body of experimental and theoretical results provides additional support for nonadiabatic excitation/relaxation models based on strong NO−metal coupling and electron−hole pair-mediated excitation of NO internal degrees of freedom.[16,31−33,60]

■ ASSOCIATED CONTENT

Supporting Information

The Supporting Information is available free of charge at https://pubs.acs.org/doi/10.1021/acs.jpcc.0c07861.

Sample LIF spectrum of the incident NO/H_2 seeded beam, revealing a 1−2 K rotational temperature and <6.6 × 10^{-4} fraction in the excited ($^2\Pi_{3/2}$) spin orbit state (PDF)

https://dx.doi.org/10.1021/acs.jpcc.0c07861
J. Phys. Chem. C 2021, 125, 341−353

AUTHOR INFORMATION

Corresponding Author

David J. Nesbitt − *JILA, National Institute of Standards and Technology and University of Colorado, Boulder, Colorado 80309, United States; Department of Physics and Department of Chemistry, University of Colorado, Boulder, Colorado 80309, United States;* orcid.org/0000-0001-5365-1120; Email: djn@jila.colorado.edu

Authors

Amelia Zutz − *JILA, National Institute of Standards and Technology and University of Colorado, Boulder, Colorado 80309, United States; Research Electro-Optics, Inc, Boulder, Colorado 80301, United States*

Kirk A. Peterson − *Department of Chemistry, Washington State University, Pullman, Washington 99164, United States;* orcid.org/0000-0003-4901-3235

Complete contact information is available at: https://pubs.acs.org/10.1021/acs.jpcc.0c07861

Notes

The authors declare no competing financial interest.

ACKNOWLEDGMENTS

This work has been supported primarily by the Air Force Office of Scientific Research (FA9550-15-1-0090), with additional funds for apparatus development provided by the National Science Foundation: Chemical, Structure, Dynamics and Mechanisms-A Program (CHE-1665271) and Physics Frontier Center (PHY-1734006).

REFERENCES

(1) Rettner, C. T.; Fabre, F.; Kimman, J.; Auerbach, D. J. Observation of Direct Vibrational-Excitation in Gas-Surface Collisions-NO on Ag(111). *Phys. Rev. Lett.* **1985**, *55*, 1904−1907.

(2) Bartels, N.; Golibrzuch, K.; Bartels, C.; Chen, L.; Auerbach, D. J.; Wodtke, A. M.; Schafer, T. Dynamical Steering in an Electron Transfer Surface Reaction: Oriented NO(v = 3, 0.08 < E-I < 0.89 eV) Relaxation in Collisions with a Au(111) Surface. *J. Chem. Phys.* **2014**, *140*, No. 054710.

(3) Bartels, N.; Golibrzuch, K.; Bartels, C.; Chen, L.; Auerbach, D. J.; Wodtke, A. M.; Schafer, T. Observation of Orientation-Dependent Electron Transfer in Molecule-Surface Collisions. *Proc. Natl. Acad. Sci. U.S.A.* **2013**, *110*, 17738−17743.

(4) Hou, H.; Rettner, C. T.; Auerbach, D. J.; Huang, Y.; Gulding, S. J.; Wodtke, A. M. The Interaction of Highly Vibrationally Excited Molecules with Surfaces: Vibrational Relaxation and Reaction of NO(v) at Cu(111) and O/Cu(111). *Faraday Discuss.* **1999**, *113*, 181−200.

(5) Huang, Y.; Wodtke, A. M.; Hou, H.; Rettner, C. T.; Auerbach, D. J. Observation of Vibrational Excitation and Deexcitation for NO(v = 2) Scattering from Au(111): Evidence for Electron-Hole-Pair Mediated Energy Transfer. *Phys. Rev. Lett.* **2000**, *84*, 2985−2988.

(6) White, J. D.; Chen, J.; Matsiev, D.; Auerbach, D. J.; Wodtke, A. M. Conversion of Large-Amplitude Vibration to Electron Excitation at a Metal Surface. *Nature* **2005**, *433*, 503−505.

(7) Wodtke, A. M.; Huang, Y. H.; Auerbach, D. J. Interaction of NO(v = 12) with LiF(001): Evidence for Anomalously Large Vibrational Relaxation Rates. *J. Chem. Phys.* **2003**, *118*, 8033−8041.

(8) Rahinov, I.; Cooper, R.; Matsiev, D.; Bartels, C.; Auerbach, D. J.; Wodtke, A. M. Quantifying the Breakdown of the Born-Oppenheimer Approximation in Surface Chemistry. *Phys. Chem. Chem. Phys.* **2011**, *13*, 12680−12692.

(9) Huang, Y. H.; Rettner, C. T.; Auerbach, D. J.; Wodtke, A. M. Vibrational Promotion of Electron Transfer. *Science* **2000**, *290*, 111−114.

(10) Larue, J. L.; White, J. D.; Nahler, N. H.; Liu, Z.; Sun, Y.; Pianetta, P. A.; Auerbach, D. J.; Wodtke, A. M. The Work Function of Submonolayer Cesium-Covered Gold: A Photoelectron Spectroscopy Study. *J. Chem. Phys.* **2008**, *129*, No. 024709.

(11) Cooper, R.; Rahinov, I.; Li, Z. S.; Matsiev, D.; Auerbach, D. J.; Wodtke, A. M. Vibrational Overtone Excitation in Electron Mediated Energy Transfer at Metal Surfaces. *Chem. Sci.* **2010**, *1*, 55−61.

(12) Geweke, J.; Shirhatti, P. R.; Rahinov, I.; Bartels, C.; Wodtke, A. M. Vibrational Energy Transfer near a Dissociative Adsorption Transition State: State-to-State Study of HCl Collisions at Au(111). *J. Chem. Phys.* **2016**, *145*, No. 054709.

(13) Matsiev, D.; Li, Z. S.; Cooper, R.; Rahinov, I.; Bartels, C.; Auerbach, D. J.; Wodtke, A. M. On the Temperature Dependence of Electronically Non-Adiabatic Vibrational Energy Transfer in Molecule-Surface Collisions. *Phys. Chem. Chem. Phys.* **2011**, *13*, 8153−8162.

(14) Born, M.; Oppenheimer, R. Quantum Theory of Molecules. *Ann. Phys.* **1927**, *84*, 457−484.

(15) Gadzuk, J. W. Inelastic Resonance Scattering, Tunneling, and Desorption. *Phys. Rev. B* **1991**, *44*, 13466−13477.

(16) Gadzuk, J. W.; Holloway, S. Vibrational-Excitation in Gas-Surface Collisions. *Phys. Rev. B* **1986**, *33*, 4298−4300.

(17) Landman, U.; Kleiman, G. G.; Cleveland, C. L.; Kuster, E.; Barnett, R. N.; Gadzuk, J. W. Hindered and Modulated Rotations of Adsorbed Diatomic-Molecules-States and Spectra. *Phys. Rev. B* **1984**, *29*, 4313−4326.

(18) Watts, E. K.; Siders, J. L. W.; Sitz, G. O. Vibrational Excitation of NO Scattered from Cu(110). *Surf. Sci.* **1997**, *374*, 191−196.

(19) Mantell, D. A.; Maa, Y. F.; Ryali, S. B.; Haller, G. L.; Fenn, J. B. Distribution of Internal Energy in NO Vibrationally Excited by a Hot Platinum Surface. *J. Chem. Phys.* **1983**, *78*, 6338−6339.

(20) Asscher, M.; Guthrie, W. L.; Lin, T. H.; Somorjai, G. A. Energy Redistribution among Internal States of Nitric-Oxide Molecules Upon Scattering from Pt(111) Crystal-Surface. *J. Chem. Phys.* **1983**, *78*, 6992−7004.

(21) Ran, Q.; Matsiev, D.; Auerbach, D. J.; Wodtke, A. M. Observation of a Change of Vibrational Excitation Mechanism with Surface Temperature: HCl Collisions with Au(111). *Phys. Rev. Lett.* **2007**, *98*, No. 237601.

(22) Zutz, A.; Nesbitt, D. J. Quantum-State-Resolved Scattering of NO($^2\Pi_{1/2}$) from Hot Molten Au(Liq): On the Role of Thermal Electron-Hole Pairs in Vibrational Excitation Dynamics. *J. Phys. Chem. C* **2018**, *122*, 17161−17169.

(23) Ziemkiewicz, M. P.; Roscioli, J. R.; Nesbitt, D. J. State-to-State Dynamics at the Gas-Liquid Metal Interface: Rotationally and Electronically Inelastic Scattering of NO[$^2\Pi_{1/2}$(0.5)] from Molten Gallium. *J. Chem. Phys.* **2011**, *134*, 234703−234714.

(24) Manning, M.; Morgan, J. A.; Castro, D. J.; Nathanson, G. M. Examination of Liquid Metal Surfaces through Angular and Energy Measurements of Inert Gas Collisions with Liquid Ga, In, and Bi. *J. Chem. Phys.* **2003**, *119*, 12593−12604.

(25) Ronk, W. R.; Kowalski, D. V.; Manning, M.; Nathanson, G. M. Inert Gas Scattering from Molten Metals: Probing the Stiffness and Roughness of the Surfaces of Atomic Liquids (Vol 104, Pg 4842, 1996). *J. Chem. Phys.* **1996**, *105*, 4397.

(26) Werner, H.-J.; Knowles, P. J.; Lindh, R.; Manby, F. R.; Schütz, M.; Celani, P.; Korona, T.; Mitrushenkov, A.; Rauhut, G.; Adler, T. B.;et al. *Molpro, a Package of Ab Initio Programs*, version 2009.1, 2009. Http://Www.Molpro.Net.

(27) Zutz, A.; Nesbitt, D. J. Nonadiabatic Spin-Orbit Excitation Dynamics in Quantum-State-Resolved NO $^2\Pi_{1/2}$ Scattering at the Gas-Room Temperature Ionic Liquid Interface. *J. Phys. Chem. C* **2015**, *119*, 8596−8607.

(28) Alcock, C. B.; Itkin, V. P.; Horrigan, M. K. Vapour Pressure Equations for the Metallic Elements: 298−2500 K. *Can. Metall. Q.* **2013**, *23*, 309−313.

(29) Houston, P. L. *Chemical Kinetics and Reaction Dynamics*; McGraw-Hill: New York, 2001.
(30) Ziemkiewicz, M.; Wojcik, M.; Nesbitt, D. J. Direct Evidence for Nonadiabatic Dynamics in Atom Plus Polyatom Reactions: Crossed-Jet Laser Studies of F + D_2O → DF + OD. *J. Chem. Phys.* **2005**, *123*, 224301−224309.
(31) Shenvi, N.; Roy, S.; Tully, J. C. Nonadiabatic Dynamics at Metal Surfaces: Independent-Electron Surface Hopping. *J. Chem. Phys.* **2009**, *130*, 174107−174118.
(32) Shenvi, N.; Roy, S.; Tully, J. C. Dynamical Steering and Electronic Excitation in NO Scattering from a Gold Surface. *Science* **2009**, *326*, 829−832.
(33) Wodtke, A. M.; Tully, J. C.; Auerbach, D. J. Electronically Non-Adiabatic Interactions of Molecules at Metal Surfaces: Can We Trust the Born-Oppenheimer Approximation for Surface Chemistry? *Int. Rev. Phys. Chem.* **2004**, *23*, 513−539.
(34) Golibrzuch, K.; Shirhatti, P. R.; Altschaffel, J.; Rahinov, I.; Auerbach, D. J.; Wodtke, A. M.; Bartels, C. State-to-State Time-of-Flight Measurements of NO Scattering from Au(111): Direct Observation of Translation-to-Vibration Coupling in Electronically Nonadiabatic Energy Transfer. *J. Phys. Chem. A* **2013**, *117*, 8750−8760.
(35) Large, T. A. L.; Nesbitt, D. J. Low Energy Co Scattering at the Gas-Liquid Interface: Experimental/Theoretical Evidence for a Novel Sub-Thermal Impulsive Scattering (Stis) Channel. *J. Phys. Chem. C* **2020**, No. 305.
(36) Perkins, B. G.; Haber, T.; Nesbitt, D. J. Quantum State-Resolved Energy Transfer Dynamics at Gas-Liquid Interfaces: IR Laser Studies of CO_2 Scattering from Perfluorinated Liquids. *J. Phys. Chem. B* **2005**, *109*, 16396−16405.
(37) Perkins, B. G.; Nesbitt, D. J. Stereodynamics in State-Resolved Scattering at the Gas-Liquid Interface. *Proc. Nat. Acad. Sci. U.S.A.* **2008**, *105*, 12684−12689.
(38) Perkins, B. G.; Nesbitt, D. J. Toward 3d Quantum State-Resolved Collision Dynamics at the Gas-Liquid Interface: Theoretical Investigation of Incident Angle. *J. Phys. Chem. A* **2009**, *113*, 4613−4625.
(39) Perkins, B. G.; Nesbitt, D. J. High Resolution Dopplerimetry of Correlated and Quantum State-Resolved CO_2 Scattering Dynamics at the Gas-Liquid Interface. *Phys. Chem. Chem. Phys.* **2010**, *12*, 14292−14308.
(40) Jacobs, D. C.; Kolasinski, K. W.; Madix, R. J.; Zare, R. N. Rotational Alignment of NO from Pt(111)-Inelastic-Scattering and Molecular Desorption. *J. Chem. Soc., Faraday Trans. 2* **1989**, *85*, 1325−1335.
(41) Jacobs, D. C.; Kolasinski, K. W.; Madix, R. J.; Zare, R. N. Rotational-Dynamics of Desorption and Inelastic-Scattering for the NO/Pt(111) System. *J. Vac. Sci. Technol., A* **1989**, *7*, 1871−1877.
(42) Rutkowski, M.; Wetzig, D.; Zacharias, H.; Gross, A. Rotational and Vibrational Population of D_2 Desorbing from Sulfur-Covered Pd(100). *Phys. Rev. B* **2002**, *66*, No. 115405.
(43) Wetzig, D.; Rutkowski, M.; Zacharias, H.; Gross, A. Vibrational and Rotational Population Distribution of D_2 Associatively Desorbing from Pd(100). *Phys. Rev. B* **2001**, *63*, No. 205412.
(44) Stewart, G. R. Measurement of Low-Temperature Specific-Heat. *Rev. Sci. Instrum.* **1983**, *54*, 1−11.
(45) Herzberg, G. *Molecular Spectra and Molecular Structure: Spectra of Diatomic Molecules*, reprint edition; Krieger Publishing Company: Florida, 1950.
(46) Bowman, J. M.; Gossage, J. L. Rotational Cooling of Rigid Rotors Desorbed from Flat Surfaces. *Chem. Phys. Lett.* **1983**, *96*, 481−484.
(47) Kay, B. D.; Raymond, T. D.; Coltrin, M. E. Observation of Direct Multiquantum Vibrational-Excitation in Gas-Surface Scattering-NH_3 on Au(111). *Phys. Rev. Lett.* **1987**, *59*, 2792−2794.
(48) Huber, K. P.; Herzberg, G. *Molecular Spectra and Molecular Structure: Constants of Diatomic Molecules*; Van Nostrand Reinhold: New York, 1979.
(49) Wodtke, A. M.; Matsiev, D.; Auerbach, D. J. Energy Transfer and Chemical Dynamics at Solid Surfaces: The Special Role of Charge Transfer. *Prog. Surf. Sci.* **2008**, *83*, 167−214.
(50) Peterson, K. A.; Adler, T. B.; Werner, H. J. Systematically Convergent Basis Sets for Explicitly Correlated Wavefunctions: The Atoms H, He, B-Ne, and Al-Ar. *J. Chem. Phys.* **2008**, *128*, No. 084102.
(51) Kendall, R. A.; Dunning, T. H.; Harrison, R. J. Electron-Affinities of the 1st-Row Atoms Revisited-Systematic Basis-Sets and Wave-Functions. *J. Chem. Phys.* **1992**, *96*, 6796−6806.
(52) Woon, D. E.; Dunning, T. H. Gaussian-Basis Sets for Use in Correlated Molecular Calculations .5. Core-Valence Basis-Sets for Boron through Neon. *J. Chem. Phys.* **1995**, *103*, 4572−4585.
(53) Peterson, K. A. Correlation Consistent Basis Sets. http://tyr0.chem.wsu.edu/~kipeters/basis.html (accessed August, 2020).
(54) Peterson, K. A.; Dunning, T. H. Accurate Correlation Consistent Basis Sets for Molecular Core-Valence Correlation Effects: The Second Row Atoms Al-Ar, and the First Row Atoms B-Ne Revisited. *J. Chem. Phys.* **2002**, *117*, 10548−10560.
(55) Wilson, A. K.; Woon, D. E.; Peterson, K. A.; Dunning, T. H. Gaussian Basis Sets for Use in Correlated Molecular Calculations. IX. The Atoms Gallium through Krypton. *J. Chem. Phys.* **1999**, *110*, 7667−7676.
(56) Govind, N.; Wang, Y. A.; Carter, E. A. Electronic-Structure Calculations by First-Principles Density-Based Embedding of Explicitly Correlated Systems. *J. Chem. Phys.* **1999**, *110*, 7677−7688.
(57) Huang, C.; Pavone, M.; Carter, E. A. Quantum Mechanical Embedding Theory Based on a Unique Embedding Potential. *J. Chem. Phys.* **2011**, *134*, 11.
(58) Huang, P.; Carter, E. A. Advances in Correlated Electronic Structure Methods for Solids, Surfaces, and Nanostructures. *Annu. Rev. Phys. Chem.* **2008**, *59*, 261−290.
(59) Herzberg, G. *Spectra and Molecular-Structure. Vol. 2. Infrared and Raman Spectra of Polyatomic Molecules*; van Nostrand Reinhold Co.: Toronto, 1945.
(60) Tully, J. C. The Dynamics of Adsorption and Desorption. *Surf. Sci.* **1994**, *299−300*, 667−677.

https://dx.doi.org/10.1021/acs.jpcc.0c07861
J. Phys. Chem. C 2021, 125, 341−353